PCCP

Accepted Manuscript

ROYAL SOCIETY OF CHEMISTRY

www.rsc.org/pccp

Journal Name

ARTICLE

Fabrication of Superhydrophilic-underwater Superoleophobic Inorganic anti-corrosive Membranes for High-efficiency oil/water Separation

Received 00th January 20xx,
Accepted 00th January 20xx

DOI: 10.1039/x0xx00000x

www.rsc.org/

Luyan Liu,[a] Chen Chen,[a] Siyu Yang,[a] Hua Xie,[a] MaoGang Gong*[b] and Xiaoliang Xu*[a]

The issue of oil/water separation has recently become a global concern due to the frequency of oil spills and the increase in industrial waste water. Thus, membrane-based materials with unique wettability are desired to separate both from the mixture. Nevertheless, the fabrication of energy efficient and stable membranes appropriate for the separation process remains challenging. Synergistic superhydrophilic-underwater superoleophobic inorganic membranes were inventively created by a maneuverable galvanic displacement reaction on copper mesh herein. The "water-loving" meshes were then used to study gravity driven oil-water separation, where separation efficiency (the ratio of content of oil remaining above the membrane after separation process to the content of oil in original mixture) up to 97% was achieved for various oil-water mixtures, and furthermore the wetting properties, separating performances maintained without further attenuation after exposed in corrosive environment. Notably, the "repelling-oil" mode can switch to superhydrophobic mode which acts as a supplementary "absorbing-oil slick" material floating above water surface with potentials in tackling oil slick clean-up issue for the former mode which possessing better "separation ability" and meanwhile the original "repelling-oil" state can be reimplemented with facility. The involved "one-cyclic tranformation course" abandon extra chemical addition with novelty. This facile and green route presented here acts as an excellent test for fabricating a dual-function membrane with the potential for efficient oil-water separation even in harsh environment and off shore oil spill cleanup.

1. Introduction

Oil/water separation has been a global task due to frequent oil leakage pollution, increasing release of industrial oily wastewater, as well as the resulting tougher regulations concerning oily industrial wastewater discharges.[1-3] Therefore, there exists an increasing demand for the development of inexpensive and effective approaches for addressing this serious issue. Conventional separation methods, such as oil skimmers, centrifuges, floatation techniques, coalescers as well as air flotations are limited by a series of shortages, such as relative low separation efficiency, vast energy costs, complex separation equipment and secondary pollution.[4-8] Thus, novel functional materials with efficient, environmentally-friendly, and cost-effective properties are urgently desired for their stability and longevity in oil/water separation process. Enlightened by the fact that immiscible oil-water mixtures commonly exist as an interfacial phenomenon, [9, 10] the materials with preferential wetting toward oil or water can be synthesized to act as the primary tool in conquering this thorny issue.

So far, it is well documented that the introduction of superhydrophobic and superoleophilic materials (also termed as "oil-loving" type of materials) are able to achieve oil/water separation effectively.[11-15] These materials, such as inorganic materials,[16-19] organic polymer materials,[20-22] or some organic/inorganic hybrid materials,[15, 23, 24] have been widely used to achieve the separating behavior showing that the oil phase spreads and penetrates through the materials easily while the water phase is simultaneously repelled. Despite all this, some drawbacks could not be ignored - as water generally has a higher density than oils, it tends to form a barrier layer which prevents oils from permeating. More importantly, these "oil-loving" materials membranes are easily fouled, blocked up and even damaged by some adhered oils during the separation process, thus resulting in gradually decreased oil/water separation efficiency and further limiting their practical applications.[25, 26] Recently, inspired by an outstanding anti-wetting behavior of oil droplets situated on the fish scale in aqueous media, the materials with superhydrophilic-underwater superoleophobic properties (named as "water-loving" types of materials) have caught our attention and presented an alternative route to solve an abundant of the aforementioned puzzles.[27-29] With this knowledge in mind, a variety of preparation methods have been proposed sequentially to achieve these fantastic substrates, such as sol-gel method, direct oxidation, polymerization, Layer-by-Layer coating, hydrothermal treatment and chemical vapor deposition. Until now, various materials such as ZnO,[30] TiO_2,[31] Zeolites,[32] silica,[33] $CaCO_3$,[34] $Cu(OH)_2$,[35] hydrogels,[36] polymer membranes,[37] graphene

[a] Key Laboratory of Strongly-Coupled Quantum Matter Physics，Chinese Academy of Sciences，School of Physical Sciences, University of Science and Technology of China, Hefei 230026, PR China. *Corresponding author with E-mail: xlxu@ustc.edu.cn; Tel: +86 551 6360574(XL.Xu)
[b] Department of Physics and Astronomy, University of Kanas, Lawrence, KS 66045, United States. *Corresponding author with E-mail: gmg@ku.edu; Tel:+1 785-8645151 (MG. Gong)

† Electronic supplementary information (ESI) available: water and oil contact angle on the inorganic membrane in air after exposed under the infrared lamp; the total XPS spectrum of the superhydrophobic Ag-coated copper film and the C1s, Ag 3d, Cu XPS spectrum respectively. SEM image of the obtained "oil-loving and water-repelling" membrane before and after annealing treatment.

oxides,[38] have been investigated in order to achieve superhydrophilic surface with good underwater-oil repelling ability. During the separation process, water phase will remain in continuous contact with the separation membrane, thus the stability of the "water-loving" membranes in harsh aqueous atmosphere such as strong acid or strong alkaline deserves more attention when referring to practical applications. Hereto, the membranes with such steady properties mainly consisted of some polymer-coated membranes which have certain weakness upon consideration of high costs and tedious preparation process, and always suffer from poor stability and become unstable under harsh conditions which occur during the separation process. For example, they would lose the original stability and states when placed in a harsh environment ,[35, 37, 39] such as high temperature. Another obstacle emerged from their weak environmental adaptability, which manifested as their swelling characteristics in a water environment or the occurrence of metamorphosis for polymeric membranes under long-term scouring by water.

An inorganic superhydrophilic membrane exhibiting good underwater-oil repellency characteristics was fabricated through a simple galvanic displacement reaction on copper mesh. The as-prepared membranes constituted from copper meshes wrapped with silver outside can effectively separate various kinds of immiscible oil/water mixtures. This separation methodology is solely based on gravity, it allows water to permeate through the film rapidly whereas the oil phase is retained above the membrane, thus proved to be an energy-efficient filter for high efficiency-oil/water separation. Separation efficiency was affected by diverse mesh numbers or types of oil and the desired high separation efficiency could be achieved when choosing the proper mesh number. Higher stability under corrosive water than previously examined inorganic films and a converse mode can both be achieved using our membrane. The thermal stability, reusability and ambient environmental stabilities is also evaluated. Interestingly, the "water-loving and oil-repelling" mode can switch to "water-repelling and oil-loving" mode by a simple exposure under infrared lamp without extra chemical modification. After this simple switching which particularly increase functionality of this membranes, the membranes can be adopted as a promising absorbing candidate to tackle the issue of "smaller scale secondly-pollution" oil slick clean-up, and demonstrates a supplementary "absorbing-oil slick" application above surface of water for the former mode which possessing better "separation ability". It's noted that the switch state can be regained to its original mode state within a short annealing time. XPS analysis indicates that this switchable transformations is originated from the adsorption and desorption of nonpolar carbon contaminants on the rough silver surface. The presented method, with multiple advantages of simple operation, low cost, brief reaction time, and environmental friendliness, could help to provide a facile and green route for fabricating a dual-function membrane with the potential for efficient oil-water separation even in harsh environments and off shore oil spill cleanup.

2. Experimental details

2.1 Materials

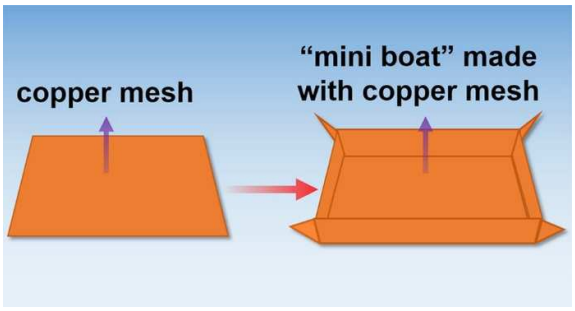

Fig. 1. Schematic Diagram showing the Fabrication of the "Mini boat"

Red-copper mesh was purchased from Sinopharm Chemical Reagent Co. Ltd (Beijing , China; the mesh number of red-copper wire was100#,120#, 150#, 180# and 200#, with the copper content of 99.8%). ethanol (C_2H_5OH, 99.0%), acetone (C_3H_6O, 99.0%), hydrochloric acid (HCl, 36.0-38.0 wt.%), sodium hydroxide, the oils and staining reagents used in the separation experiment were purchased from Sinopharm Chemical Regent Co. Ltd. (shanghai, China). Deionized water with resistivity of 18.25 MΩ was used through the entire experiment and all reagents were analytically pure and used without further purification.

2.2 Preparation of the superhydrophilic–underwater superoleophobic film with hierarchical composite structure and the transformation to the converse mode

The hierarchical structures on copper mesh were fabricated through a simple electroless galvanic displacement reaction as follows: the copper meshes were first ultrasonically degreased with acetone, ethanol and deionized water for 10 min each, then the meshes were dipped in hydrochloric acid solution for another 10 min to remove the oxides existing on surface. Next, after being dried by a stream of high purity N_2, the copper meshes with different mesh number were immersed into 0.1M $AgNO_3$ aqueous solution for a few seconds without any redundant reagents to modify surface morphology of these samples. The meshes were rinsed with large amounts of water and ethanol and blown dry. In order to complete the conversion from the superhydrophobic-underwater superoleophobic sample to superhydrophobic/superoleophilic one, the membranes were placed inside an oven containing an infrared lamp for 6 hours.

2.3 Preparation of Superhydrophobic–superoleophilic "Mini Boat"

As shown in Fig. 1, the obtained superhydrophobic copper mesh sheet (5cm × 6cm) after being exposed under the infrared lamp was enfolded into a miniature box with the size of 3.5 cm × 4.5 cm × 1.5cm. The copper mesh box was placed into a culture dish filled with water, and n-hexane was gradually added onto water surface to simulate an oil contaminant.

2.4 Characterization

Microstructures of the samples were observed using a field emission scanning electron microscopy (FESEM, JSM-6700F) with the operating voltage of 5KV. Surface chemical components were analyzed via an X-ray photoelectron spectroscope (XPS) (THERMO Corp., ESCALAB250), which is equipped with standard monochromatic Al-Kα radiation (hν = 8047.8 Ev). The static water contact angles (WCAs) and underwater oil contact angles (OCAs) were measured by the CAST 2.0 contact angle analysis system (Solon Information Technology Co. Ltd., Shanghai, China). Notably, for underwater oil wetting performance measurements, the substrates were fixed in a container which is absolutely transparent and filled with water. For oils with relative lower density than water, such as hexane, the oil droplet was released under the mesh through an inverted needle. Conversely, the oil droplet was put on it directly for oils with higher density, like 1, 2-dichloroethane. Each WCA or OCA (oil contact angle) value was averages obtained by measuring at least five different positions of the same samples and the volume of individual water droplets used for the static WCA and SA measurement was 4 μL.

3. Results and discussion

The typical surface microstructures of copper meshes with mesh number of 180# were examined by FE-SEM before and after immersion. The initial copper mesh had a micron-scale rough structure, with a wire diameter in the range of approximately 50 um and pore size of 85 um (see Fig. 2a). The surface of mesh grid was relatively smooth and no obvious submicron or nanostructures were observed in the magnified images (Fig. 2b). After immersed in $AgNO_3$ solution with a short duration time of 10 s, a silver layer was clearly observed on the mesh surface as a consequence of the electroless galvanic displacement reaction:

$$Cu_{(s)} + AgNO_{3(aq)} = Ag_{(s)} + Cu(NO_3)_{2(aq)}$$

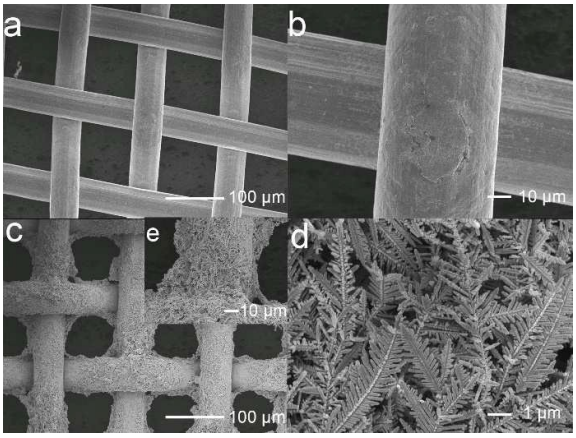

Fig. 2 SEM images of (a),(b) are the original copper mesh with low and high magnification, (c)-(e) are the Ag-coated membrane with different magnifications

Fig. 2c and its high magnification image Fig. 2e show that the mesh grids were uniformly covered by submicron or nano-structures. The local magnification image (Fig. 2d) further indicates the structure of coating layer. The same structure as "sago cycas" branch is consisted of primary-branch (trunk) with

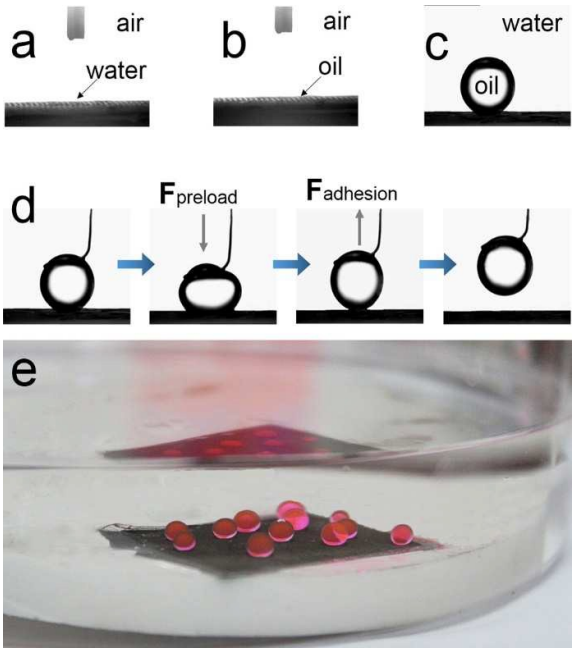

Fig. 3 Special wettability of the coated mesh. Photograph of (a) water droplet (4ul) and (b) oil droplet (1,2-dichloroethane, 4ul) on this inorganic mesh in air and (c) underwater with a contact angle of 159°.(d) a serious of photographs of the oil droplet(1,2-dichloroethane, 4ul) touching-pressed by force-leaving the membrane substrate.(e) Optical image of the 1,2-dichloroethane deposited on the superhydrophilic-underwater superolophobic copper mesh underwater

secondary-branches. These secondary branches are parallel to each other and grow at fixed angles with respect to the central trunk, whose length is around several micrometers while the diameter varies in a range of 80-90 nm. Hence, the surface of the modified copper mesh possesses amplified multi-scale roughness which is expected to own the ability to strengthen the particular wetting performances.

The wettability of a surface is mainly determined by its morphology and the surface chemical composition. The chemical composition or surface exposed groups determine the surface energy and exhibits different surface properties, hydrophobic or hydrophilic, while topographical structures can further amplify its surface property to superhydrophobicity or superhydrophilicity .[40, 41] The as-prepared inorganic membrane surfaces exhibited superamphiphilic in a solid-liquid-air three phase system with both the WCA and OCA less than 5° (Fig. 3a,b), which would be attributed to its innate hydrophilic property combining with the enhanced surface roughness. On the contrary–when immersed in a water bath, the membrane gives a CA of 159° for an oil droplet (1, 2-dichloroethane, Fig. 3 c and Fig. 3e), indicating an outstanding underwater-superoleophobic performance. In order to obtain a greater understanding of oil-repellency property, an experiment concerning adhesion ability was performed. Fig. 3d displayed the whole procedure-an oil droplet (4uL) was squeezed against membrane surface using a metal gap with an initial preload with the pressure gradually released. During the relaxation process, the oil droplet seemed to depart from the surface easily and retained its spherical shape with almost no deformation in spite of the pressure decreasing to zero, even in the case where the oil droplet was squeezed against the surface with some higher preload. This low adhesion property can prevent the mesh from fouled by oil during

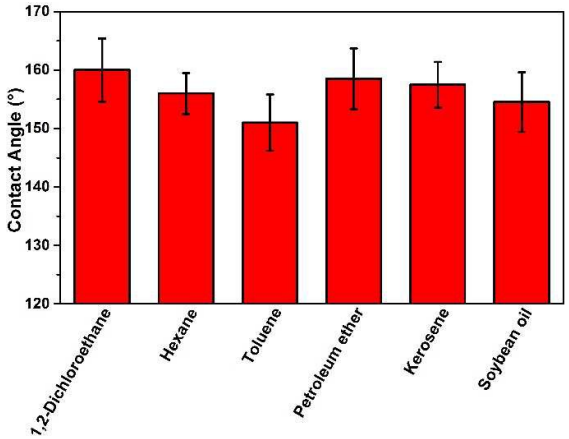

Fig.4 Contact angles of a series of typical oil droplets on the coated inorganic functional membrane in aqueous media

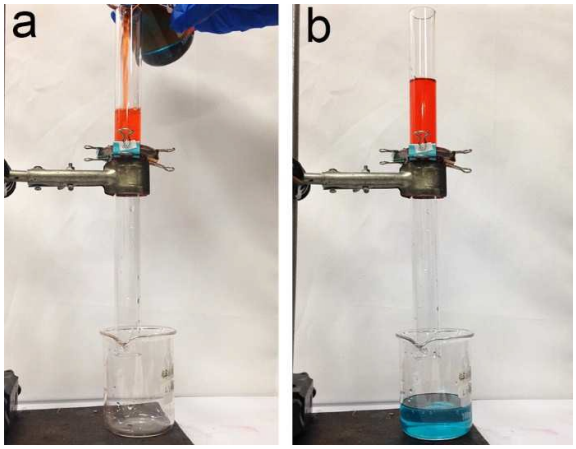

Fig.5 (a) oil/water separation by the as-prepared coated mesh. The mesh was fixed between two glass tubes and pre-wetted by a stream of water. A mixture of hexane (dyed in red) and water (dyed in blue) was poured into the upper glass tube. (b) The "water-loving" membrane allowed the water pass through while blocked the oil on top of membrane in the upper glass tube

the separation process and the combination of a large OCA with the low adhesion, endows the membrane with extraordinary underwater superoleophobic properties. The origination of this peculiar phenomenon is from the formation of a water cushion between oil droplet and solid substrate. There are trapped water molecules residing between the interspaces of the rough surface, which not only provides a strong repulsive force due to the repulsive interaction between polar (water) and non-polar (oil) molecules, but also contributes to decrease the oil-adhesion force.[39, 42] Thermal stability of the membrane is additionally examined after the membrane is heated at 350°C in a muffle furnace for 2.5 h, it maintains its original underwater superoleophobic property with oil CA of 154°. Besides, to evaluate the long-term environmental stabilities of the membrane, it is placed in air with a piece of plastic sheeting covering on surface for one week at ambient temperature. Fig. S1 shows that the underwater oil CA experiences little fluctuations in this case, which demonstrate the membrane owns stable underwater superoleophobicity in ambient environment.

Further experiments were conducted to confirm that the as-prepared copper mesh membrane also exhibited excellent underwater superoleophobic performance towards other various kinds of oils (including 1, 2-dichloroethane, toluene, petroleum ether, kerosene and soybean oil) apart from the used oil (n-hexane) mentioned above. Fig. 4 illustrates the different oil on the copper

mesh membrane and all of them are over 150°, which demonstrates as a strong proof that the as-prepared membrane own a better and more universal superhydrophilicity and underwater-superoleophobicity performance.

Table 1. Pore size and wire diameter of the initial copper mesh with different mesh numbers.

Mesh number(#)	Wire size(um)	Pore size(um)
100	100	150
120	70	140
150	60	100
180	50	90
200	50	70

The unique performance of the inorganic membranes is feasible and desirable for oil/water separation, and pictorial views of oil-water separation system used in this study are shown in Fig. 5. A mixture of n-hexane (colored with oil red)–water (colored with methylene blue) with total volume 70ml (V_{water} / V_{oil} =7:3) is poured into the upper glass tube to assess oil-water separation capability of this 180# membrane (experiments show the mesh is able to separate trace of oil ie 95% water vs 5% oil with high efficiency as well). It's worth noting that the mesh should be wetted by a stream of water prior to this separation and gravity is the only driving force for the oil/water separation. Owing to the outstanding oil/water separation ability of the prepared copper mesh, water experiencing a larger gravitational force than oil could permeate through the mesh with a high speed and flow into the under beaker while n-hexane is retained above the mesh (the separation result is exhibited as Fig. 5b).The whole separation process was accomplished within a short time (See Movie 1in supporting information) and correlative oil-water separation efficiency was calculated using equation [1][42].

$$E_{ff} = (1 - C_p / C_o) \times 100\% \qquad [1]$$

Where C_o and C_p are determined by measuring the volume of oil in original oil-water mixture and filtered mixture respectively, using a small measurement range graduated cylinder. The calculated separation efficiency measurement reached a high value of 99.2% in this case. Other oils, 1, 2-dichloroethane, toluene, petroleum ether, kerosene and soybean oil were also used in testing the efficiency of the same mesh separated from water. Fig. 6a, it shows that the separation efficiencies of coated mesh (180#) are above 97% for various oil-water mixtures, compared to no separation at all for uncoated meshes with identical mesh number. Furthermore, after separation, the film can be used repeatedly by simply rinsed with little ethanol and then dried. Over thirty repetitions, the membrane still keep stable performance without visible morphology variation as shown in Fig. S2.

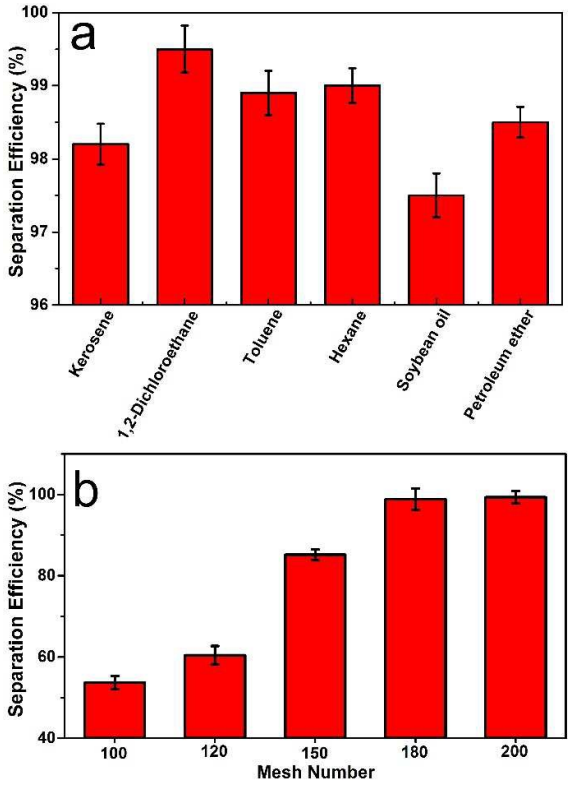

Fig. 6 (a) The separation efficiency of various of oil/water mixtures and (b) The influence of mesh number on the separation efficiency of the functional inorganic membrane

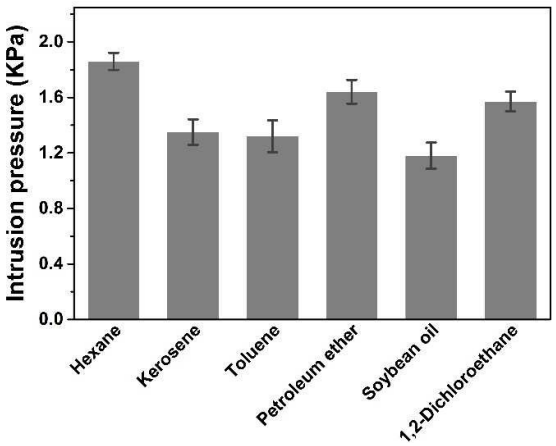

Fig. 7 The intrusion for a serious of oils

Under this oil-water separation system, four other copper mesh membranes with different kinds of pore sizes (100#, 120#, 150#, 200#) were tested as well. The space of the pores decrease when the mesh number increase (The correspondence relationship of the size and mesh number is displayed in Table 1). Fig. 6b shows the relationship between the separation efficiency and mesh number, which immersed in 0.1M $AgNO_3$ solution for 10s. It indicates that the efficiency is inversely correlated with the pore size. When the mesh number is less than 150#, the separation efficiency is lower than 70%. While, 98.8% and even higher 99.2% oil-water separation efficiency are achieved on 180# and 200#mesh, respectively. The result is plausible, because the larger pore size of the membrane (smaller mesh number) is more favourable for the permeation of water. In addition, the reduction of thickness of the trapped aqueous layer occurred, which resulted in insufficient surface tension to support much oil and further lead to a relative lower separation efficiency. It is demonstrated that the displacement deposition time has an influence on separation efficiency as well (see Fig. S3) and when the reaction time ascends above 10s, the efficiency range with a little fluctuation.

To further study the separation ability of the as-prepared meshes, the intrusion pressure of oil flowing through the coated mesh was measured, which indicated the maximum height (h_{max}) of oil that the mesh can support. The intrusion pressures for various oils were measured by pouring oil onto mesh prewetted with water to achieve the maximum height and the intrusion pressure is provided by the weight of oil, therefore, the experiment value can be obtained according to the equation below:

$$P = \rho g h_{max} \qquad [2]$$

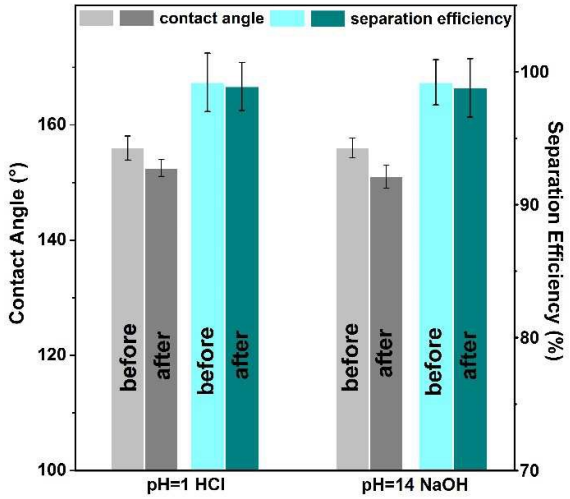

Fig. 8 Oil contact angles (left axis) and separation efficiency (right axis)of the nanostructured film before and after immersed in HCl (pH=1) and NaOH (pH=14) solutions respectively

Where **P** is the experimental intrusion pressure, **ρ** is the density of the accordingly oil, **g** means the acceleration gravity and h is as previously mentioned. Fig. 7 shows the intrusion pressures for various oils, and clearly to observe the average intrusion pressures for all these oils are above 1.0 kPa, demonstrating that our separating device has a good stability. The water flux (F) was also measured and the relevant content is displayed in SI.

In real-word application, the harsh environment are unavoidable and may result in serious consequences. For instance, in oil/water separation process, the stability of an as-prepared "water-loving" membrane film in corrosive liquids such as strong acid or strong alkaline is of vital importance. To evaluate the stability and resistance against corrosion for our membrane, a corresponding experiment was performed. Using the 180# mesh number membrane with a reaction time of 10s, we immersed it in different liquid environments for as long as 12h (in this case we adopt HCl solution together with NaOH solution whose according pH value is 1 and 14 , respectively), the oil-repellency and separation performance (here we adopt the mixture of hexane/water) of the membrane were all tested afterwards. Ecstatically to observe the membrane maintain its original underwater superoleophobic property with outstanding separation efficiency despite suffering from the immersion treatment (as displayed in Fig. 8). This result indicated an excellent solvent resistance ability, which exhibits more feasibility of application compared to polymer-dominated membranes.

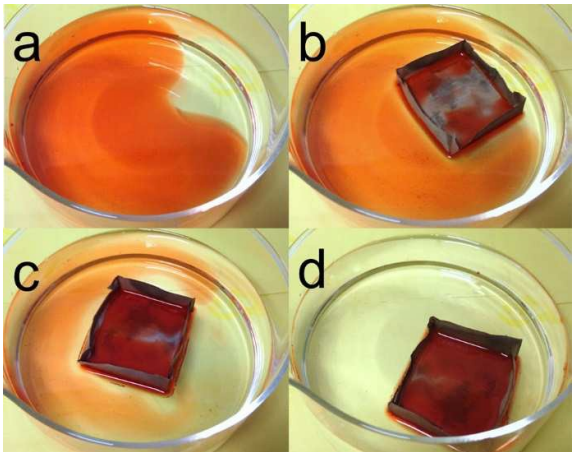

Fig.9 A photograph of the oil absorption process of the folded "infrared light-induced" superhydrophobic copper mesh boat.

Although the prepared membrane possess advantages than "oil-loving" mode, the latter can still provide a complentary application as a promising "oil-absorbing" material in tackling the issue of "smaller scale secondly-pollution" oil slick clean-up to the former. It's well documented that large numbers of superhydrophobic/superoleophilic substrates have been constructed to eliminate "polluted oil" from the contaminated water,[15, 43, 44] and the micro/nanostructure and low surface energy materials are indispensable when fabricating these surfaces. Generally, a layer of organic material is used to lower surface energy as a modifier and endow the substrate with the ability to repel water while absorbing oil scattered in the mixture. These organic modifiers are somewhat cost-ineffective and toxic to the environment. In this case, those concerns can be ignored by way of an innovative and convenient method, which can be used to create such a substrate without requiring any low-surface-energy material. As conducted in a brief manner, after being ultrasonically cleaned with large quantities of water and ethanol, the membrane used for oil/water separation process was directly placed beneath an infrared lamp for 6h. Thereafter, as can be seen from Fig. S5, the film exhibits superhydrophobicity with a WCA of 159° for water in air and in addition, the surface shows superoleophilicity with a WCA of 159° simultaneously-showing the OCA for hexane approximately to 0° (Fig. S5). To investigate the factor causing the "unmodified surface" superrepellent, the surface chemical component and their status on this Ag-coated copper mesh were examined. It was found that the nonpolar hydrocarbon organics from ambient air with low surface energy were shown to be present on the rough mesh surfaces through XPS (the relevant core-level XPS spectrum of C 1s,Cu 2p, and Ag 3d are displayed respectively in Fig. S6 and related analysis is given simultaneously, which is fully consistence with the conclusion of Liu et al[45]. The preparation of a superhydrophobic surface on silver with the rough surface for practical applications has rarely reported before[46, 47]. Considering that in the past decades, the pollution of seawater by oils is one of the most serious environmental problems worldwide and oil-absorbing materials are urgently in demand. We herein provided a solution to clean up offshore oil contamination through folding the copper mesh film into a "mini boat" to demonstrate its oil-absorbing ability. The "boat-like" mesh was placed into a culture dish filled with water, and hexane labeled with oil red dye was gradually poured into the water simulating oil pollution. It can be seen from a sequence of images shown in Fig. 9 that the "mini boat" can float freely on the water, and oil will easily permeate into it while water is simultaneously excluded.

The experiment powerfully demonstrates the tendency of the "water-loving" mode to permeate water and separate viscous and sticky oils from the mixture of the membrane, it can switch to superhydrophobic mode to permeate typical oils in oil-water mixture, and this facile-transformation can be helpful in recovering the crude oils leaked into the ocean once an oil spill has occurred. Enlightened by the work of Pan et al. [48], in order to evaluate the oil-adsorbing ability of this transformed mesh, we gradually added colored hexane into the tank containing 250 ml water with the "mini-boat" floating on the surface. Experiments show the boat can float over water surface with oil permeating inside thus leading to the incremental oil loading weight until the total volume of oil is 17.5 ml. Volume-based absorption capacity (V_{oil}/ V_{mesh}) is used to characterize the absorption capability of the organic membrane with a value of 76.1 % for hexane and the adsorbed oil is 10 times than mesh's own weight, respectively. Though these capacity values are lower than the sponge-based materials owing to their slightly inferior effective adsorbing area, [49,50] when we continuously extract the "already-adsorbed oil" from the mini-boat, it keeps for a long time adsorbing oil again even if a max adsorbing ability has been achieved just now, considering this, they still exhibit broader efficient space utilization for supplementary oil absorption.

After annealed in nitrogen atmosphere via a muffle furnace for merely 8min at 185 °C, the "oil-loving" membrane can restore to initial state which exhibits" underwater repelling-oil" phenomenon and maintain the high separation ability with slightly wearing off – 98.8% by measurement. XPS spectra in Fig. 10 illustrate element Ag, Cu, C, O and total survey spectrum of MB (the membrane before annealing treatment is denoted as MB) and MA (membrane after thermal treatment is marked as AM) corresponding to upper (1) and lower line(2), respectively. Similar spectrum with identical peak located at 368.65 and 376.64 eV in Fig. 10a suggests element Ag remains stable on membrane after annealing treatment. It demonstrates a steady and enduring property of element silver, which is consistent with little alternation of SEM morphology as shown in Fig.S6. Fig. 10b indicates a deconvolution of Cu presents

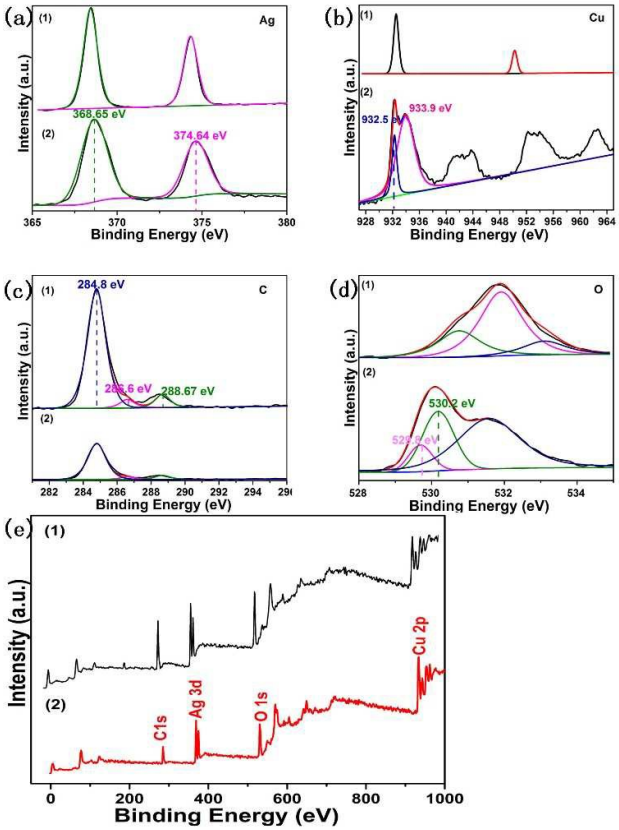

Fig. 10 XPS high-resolution spectra of (a) Ag 3d, (b) Cu 2p,(c) C 1s, (d) O 1s and (e) total XPS survey spectra. Among them, (1) belong to the spectrum before annealing treatment and (2) correspond to the annealed one.

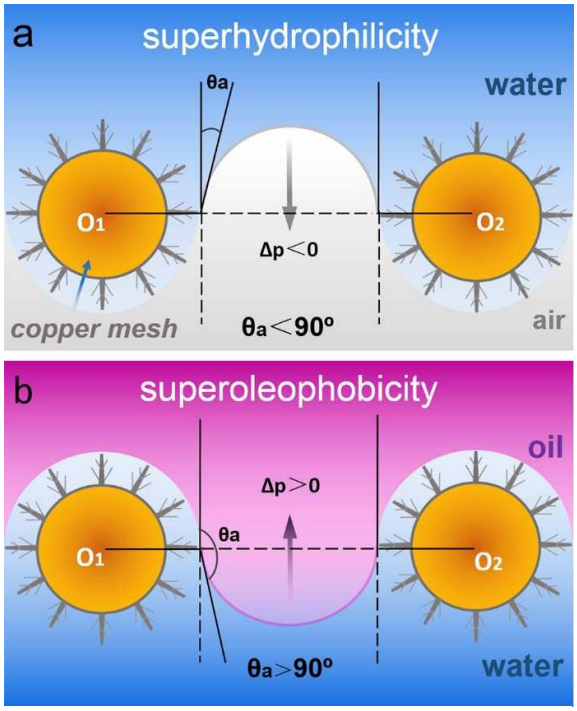

Fig .11 Schematic diagram of the water-oil wetting process: (a) Water will permeate through the membrane in air because $\Delta P < 0$. (b) Oil can stay above the membrane as to $\Delta P > 0$. In the figure, O_1 and O_2 are the cross-section center of the copper mesh

two typical peaks centered at 932.5 and 933.9 eV corresponding to Cu_2O and CuO respectively, [51,52] which is attributed to the thermal oxidation of Cu after annealing. C 1s peak intensity of MA demonstrated in Fig. 10c is in accordance with MB apart from obvious decline of intensity, it is due to the thermal decomposition of ambient airborne organic compounds exsiting on surface. O 1s spectrum of MA is resolved into two components centered at 529.8 and 530.2eV, corresponding to CuO and Cu_2O. While the peak at 531.6eV may be attributed to chemisorbed oxygen.[53] To compare the XPS spectra between MA and MB, it is noted that the organic contaminations absorbed on surface of EM has decomposed via the thermal annealing. The sole alternation of surface free energy rather than morphology (Fig. S7) endows the surface with ability to recover to original state without functional attenuation.

To understand the oil-water separation mechanism of this "water-loving" copper mesh membrane, we model the water and

oil wetting process in Fig. 11. The intrusion pressure (denoted as ΔP), can be viewed below:[54]

$$\Delta P = \frac{2\gamma}{R} = -l\gamma(\cos\theta_a)/A \quad [3]$$

Where γ means the surface tension, R is the radius of the menisus, *l* means the mesh pore's circumference, θ_a represents the advancing contact angle of oil drop on the underwater surface and A is the cross-section area of the pore. Generally speaking, for the liquid situated on surface of the membrane, transformation from Cassie to the Wenzel state cannot be realized with ease until the intrinsic advancing angle θ_a of the liquid is exceeded, which also means "the intrusion pressure"– ΔP must be conquered simultaneously. Concerning the superhydrophilic membrane placed in air, ΔP <0 can be concluded from the equation 3 when considering the behavior that water spreading quickly as soon as it dropped on the surface (θ_a ~ 0°), thus the film has no ability to support any pressure, as shown in Fig. 11a. Conversely, when the film was wetted by water to form a layer water environment in advance, the trapped water existed in the micro-nanostructures had the power to strengthen the oil-repellency performance. The retention of oil above the membrane leads to θ_a >90°.As a consequence, it is taken for granted that ΔP >0 for oil droplet in this special oil-water-solid three phase system. (Fig. 11b) Oil cannot permeate through the film spontaneously owning to the pressure sustained by the membrane and therefore an oil/water mixture can be well separated by this prepared "water-loving" membrane.

Conclusions

In summary, this work has demonstrated a superhydrophilic inorganic membrane with underwater-oil repellency for the application of oil/water separation, which can be easily fabricated by a facile electroless galvanic displacement reaction on copper mesh with various sizes. An outstanding oil/water separation efficiency reach up to 99% was achieved using the coated mesh with mesh number of 200# and the efficiency was found to be correlated with the mesh number and oil type. Moreover, outstanding anti-corrosion behavior, thermal stability, reusability and ambient environmental stabilities confirm that the coated meshes are highly stable even suffering from the harsh environments. After remaining exposed under an infrared lamp for several hours, the membrane would possess superhydrophobic ability without any low-surface-energy materials or volatile organic solvents used to demonstrate a supplementary "absorbing-oil slick" application above surface of water for the former mode which possessing better "separation ability". In addition, the recovery to initial state was implemented without complex operation to complete a cyclic process. This facile, easy-to-control and green fabrication process combined with distinct property makes it an ideal candidate for application in industry and daily life, such as separation of living waste oil or retrieving oil leakage in the ocean.

Acknowledgements

This work is supported by the National Natural Science Foundation of China (no.51272246, no.11304173) and Scientific and Technological Research Foundation of Anhui Province, China (no. 12010202035).

Notes and references

1 J. Zhang and S. Seeger, *Advanced Functional Materials*, 2011, **21**, 4699-4704.
2 N. Liu, Y. Chen, F. Lu, Y. Cao, Z. Xue, K. Li, L. Feng and Y. Wei, *Chemphyschem : a European journal of chemical physics and physical chemistry*, 2013, **14**, 3489-3494.
3 L. Zhang, Y. Zhong, D. Cha and P. Wang, *Scientific reports*, 2013,**3**, 2326-2330.
4 W. Zhang, Z. Shi, F. Zhang, X. Liu, J. Jin and L. Jiang, *Advanced materials*, 2013, **25**, 2071-2076.
5 L. Yang, A. Thongsukmak, K. K. Sirkar, K. B. Gross and G. Mordukhovich, *Journal of Membrane Science*, 2011, **378**, 138-148.
6 G. Gutierrez, A. Lobo, J. M. Benito, J. Coca and C. Pazos, *Journal of hazardous materials*, 2011, **185**, 1569-1574.
7 M. M. Pendergast and E. M. V. Hoek, *Energy & Environmental Science*, 2011, **4**, 1946-1971.
8 D. Rana and T. Matsuura, *Chemical reviews*, 2010, **110**, 2448 2471.
9 B. Wang, W. Liang, Z. Guo and W. Liu, *Chemical Society reviews*, 2015, **44**, 336-361.
10 S. Pan, R. Guo and W. Xu, *AIChE Journal*, 2014, **60**, 2752-2756.
11 W. Liang and Z. Guo, *RSC Advances*, 2013, **3**, 16469-16474.
12 B. Wang and Z. Guo, *Chemical communications*, 2013, 49, 9416-9418.
13 A. Li, H.-X. Sun, D.-Z. Tan, W.-J. Fan, S.-H. Wen, X.-J. Qing, G.-X. Li, S.-Y. Li and W.-Q. Deng, *Energy & Environmental Science*, 2011, **4**, 2062-2065.
14 S. J. Maguire-Boyle and A. R. Barron, *Journal of Membrane Science*, 2011, **382**, 107-115.

15 C. R. Crick, J. A. Gibbins and I. P. Parkin, *Journal of Materials Chemistry A*, 2013, **1**, 5943-5948.
16 X. Jin, B. Shi, L. Zheng, X. Pei, X. Zhang, Z. Sun, Y. Du, J. H. Kim, X. Wang, S. Dou, K. Liu and L. Jiang, *Advanced Functional Materials*, 2014, **24**, 2721-2726.
17 D. Zang, C. Wu, R. Zhu, W. Zhang, X. Yu and Y. Zhang, *Chemical communications*, 2013, **49**, 8410-8412.
18 C. Gao, Z. Sun, K. Li, Y. Chen, Y. Cao, S. Zhang and L. Feng, *Energy & Environmental Science*, 2013, **6**, 1147-1151.
19 K. Li, J. Ju, Z. Xue, J. Ma, L. Feng, S. Gao and L. Jiang, *Nature communications*, 2013, **4**, 2276-2282.
20 Y. Cao, Y. Chen, N. Liu, X. Lin, L. Feng and Y. Wei, *J. Mater. Chem. A*, 2014, **2**, 20439-20443.
21 X. Zhou, Z. Zhang, X. Xu, F. Guo, X. Zhu, X. Men and B. Ge, *ACS applied materials & interfaces*, 2013, **5**, 7208-7214.
22 N. Liu, X. Lin, W. Zhang, Y. Cao, Y. Chen, L. Feng and Y. Wei, *Scientific reports*, 2015, **5**, 9688-9693.
23 X. Zhang, Z. Li, K. Liu and L. Jiang, *Advanced Functional Materials*, 2013, **23**, 2881-2886.
24 Z. Shi, W. Zhang, F. Zhang, X. Liu, D. Wang, J. Jin and L. Jiang, *Advanced materials*, 2013, **25**, 2422-2427.
25 C. Wang, T. Yao, J. Wu, C. Ma, Z. Fan, Z. Wang, Y. Cheng, Q. Lin and B. Yang, *ACS applied materials & interfaces*, 2009, **1**, 2613-2617.
26 Y. Wang, S. Tao and Y. An, *J. Mater. Chem. A*, 2013, **1**, 1701-1708.
27 M. N. Kavalenka, A. Hopf, M. Schneider, M. Worgull and H. Hölscher, *RSC Advances*, 2014, **4**, 31079-31083.
28 J. Li, H. M. Cheng, C. Y. Chan, P. F. Ng, L. Chen, B. Fei and J. H. Xin, *RSC Adv.*, 2015, **5**, 51537-51541.
29 M. Nosonovsky, *Nature*, 2011, **477**, 412-413.
30 D. Tian, X. Zhang, Y. Tian, Y. Wu, X. Wang, J. Zhai and L. Jiang, *Journal of Materials Chemistry*, 2012, **22**, 19652-19657.
31 Y. Sawai, S. Nishimoto, Y. Kameshima, E. Fujii and M. Miyake, *Langmuir : the ACS journal of surfaces and colloids*, 2013, **29**, 6784-6789.
32 J. Zeng and Z. Guo, *Colloids and Surfaces A: Physicochemical and Engineering Aspects*, 2014, **444**, 283-288.
33 H. C. Yang, J. K. Pi, K. J. Liao, H. Huang, Q. Y. Wu, X. J. Huang and Z. K. Xu, *ACS applied materials & interfaces*, 2014, **6**, 12566-12572.
34 P. C. Chen and Z. K. Xu, *Scientific reports*, 2013, **3**, 2776-2781.
35 Z. Cheng, H. Lai, Y. Du, K. Fu, R. Hou, C. Li, N. Zhang and K. Sun, *ACS applied materials & interfaces*, 2014, **6**, 636-641.
36 C. Teng, X. Lu, G. Ren, Y. Zhu, M. Wan and L. Jiang, *Advanced Materials Interfaces*, 2014, **1**.
37 W. Zhang, Y. Zhu, X. Liu, D. Wang, J. Li, L. Jiang and J. Jin, *Angewandte Chemie*, 2014, **53**, 856-860.
38 Y. Dong, J. Li, L. Shi, X. Wang, Z. Guo and W. Liu, *Chemical communications*, 2014, **50**, 5586-5589.
39 L. Zhang, Z. Zhang and P. Wang, *NPG Asia Materials*, 2012, **4**, e8.
40 K. Seo, M. Kim and D. H. Kim, *Carbon*, 2014, **68**, 583-596.
41 X. Zhu, Z. Zhang, X. Men, J. Yang, K. Wang, X. Xu, X. Zhou and Q. Xue, *Journal of Materials Chemistry*, 2011, **21**, 15793-15797.
42 Z. Xue, S. Wang, L. Lin, L. Chen, M. Liu, L. Feng and L. Jiang, *Advanced materials*, 2011, **23**, 4270-4273.
43 J. Song, S. Huang, Y. Lu, X. Bu, J. E. Mates, A. Ghosh, R. Ganguly, C. J. Carmalt, I. P. Parkin, W. Xu and C. M. Megaridis, *ACS applied materials & interfaces*, 2014, **6**, 19858-19865.
44 B. Wang and Z. Guo, *Applied Physics Letters*, 2013, **103**, 063704-063708.
45 P. Liu, L. Cao, W. Zhao, Y. Xia, W. Huang and Z. Li, *Applied Surface Science*, 2015, **324**, 576-583.
46 T. Ning, W. Xu and S. Lu, *Journal of colloid and interface science*, 2011, **361**, 388-396.
47 G. Wang and T. Y. Zhang, *Journal of colloid and interface science*, 2012, **377**, 438-441.
48 Q. Pan, M. Wang, *ACS applied materials & interfaces,* 2009, **1**, 420-423.
49 Turco A., C. Malitesta, G. Barillaro, A. Greco, A. Maffezzoli and E. Mazzotta, *J. Mater. Chem. A*, 2015, **3**, 17685-17696.
50 N. Chen and Q. Pan, *ACS nano*, 2013, **7**, 6875-6883.
51 She Z., Q. Li, Z. Wang, L. Li, F. Chen and J. Zhou, *ACS applied materials & interfaces*, 2012, **4**, 4348-4356.
52 Liu L., F. Xu and L. Ma, *The Journal of Physical Chemistry C*, 2012, **116**, 18722-18727.
53 Ghijsen J., L. H. Tjeng, J. van Elp, H. Eskes, J. Westerink, G. A. Sawatzky and M. T. Czyzyk, *Physical Review B*, 1988, **38**, 11322-11330.
54 J. P. Youngblood and T. J. McCarthy, *Macromolecules*, 1999, **32**, 6800-6806.